A Practical GPR Imaging Scheme for Buried Objects

Sangeeta Tarai
Electronics and Communication
Engineering
NIT, Rourkela
Rourkela, India
519ec6023@nitrkl.ac.in

Swarna Laxmi Panda
Electronics and Communication
Engineering
NIT, Rourkela
Rourkela, India
517ec1013@nitrkl.ac.in

Buddepu Santosh Kumar
Electronics and Communication
Engineering
NIT, Rourkela
Rourkela, India
519ec1005@nitrkl.ac.in

Dr. Ajit Kumar Sahoo
Electronics and Communication
Engineering
NIT, Rourkela
Rourkela, India
ajitsahoo@nitrkl.ac.in

Dr. Subrata Maiti
Electronics and Communication
Engineering
NIT, Rourkela
Rourkela, India
smaiti@nitrkl.ac.in

Abstract—**Ground penetrating radar (GPR) is one of the most effective non-destructive method for detection and identification of buried objects. The key challenges for the imaging of the buried objects are the antenna cross talk and the presence of ground bounce. The GPR imaging is more difficult in complex ground scenario which is unpredictable. For imaging of subsurface objects, an efficient and reliable signal processing scheme is essential. Here we have developed a complete imaging scheme for buried object detection. The important steps such as clutter removal, velocity analysis, migration techniques are implemented for imaging buried object. The effectiveness of the scheme is verified by processing synthetic data as well as laboratory measurements. The proposed approach can be effective for buried object detection.**

Keywords—Clutter reduction, GPR, migration, velocity estimation.

I. INTRODUCTION

GPR is a high-resolution electromagnetic sensor to investigate the Earth's shallow subsurface. It has the potential to be a strong approach to non-destructive testing in a wide variety of applications [1]. These range from measuring material characteristics such as thickness and dielectric constant to geophysical prospecting, identification of underground objects such as cables, pipelines, and mines [1], [2]. These applications require very high resolution, reduction of clutters and high-end signal processing software, and most importantly an accurate model to represent the complex GPR scenarios. The scattered field can be recorded at multiple spatial positions as the antenna moves along a straight line on the surface to create a B-scan GPR image [4].

All GPR data requires some form of pre-processing before any realistic interpretations can be attempted [1], [2]. Preprocessing GPR data is required to eliminate any static shifts caused by elevation change and time-zero drift [2]. In general, landmines are buried near the ground's surface, and which makes object detection difficult owing to the scattering from the ground's surface [4]. These can be removed by applying different clutter reduction techniques like mean removal, SVD, and PCA [3]. GPR imaging is essentially dependent on the velocity of the subsurface medium. Many different velocity estimation techniques are available in literature such as CMP based velocity spectrum method and the common offset-based hyperbola fitting method [7], [8]. One of the most commonly utilized B-scan GPR imaging

challenges are converting an unfocused GPR image to a focused one that shows the true position and size of the objects. Kirchhoff migration and frequency-wave number migration are well-known for GPR imaging [4], [5], [6].

This paper focuses on the detection of the buried objects based on imaging. The mean removal technique is used to reduce static clutter from the raw data. Then, velocity estimation using hyperbola fitting is used to obtain the media property. Finally, migration techniques such as Kirchhoff migration and frequency wave number migration are employed for imaging. The performance of these imaging algorithms is evaluated by quantifying peak signal to noise ratio (PSNR) value.
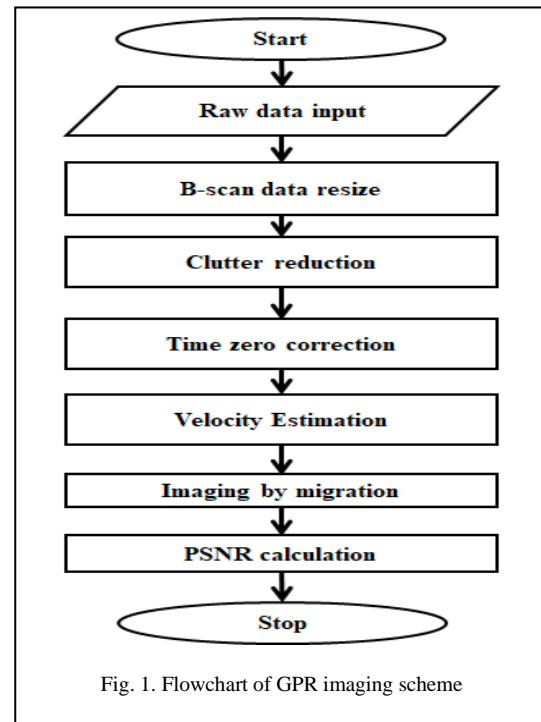
II. GPR IMAGING SCHEME

Fig. 1. Flowchart of GPR imaging scheme

The B-scan image can be formed by concatenating series of A-scans taken at regular intervals along the scan axis. The B-scan data is resized by downsampling each A-scan to achieve finer resolution. IFFT is applied to the B-scan data to convert from frequency domain to time domain.

The primary sources of interference for shallowly buried objects are antenna cross talk and ground bounce, which can be reduced using clutter reduction techniques. Time zero correction has been achieved by considering the phase center of the antenna to nullify the antenna delay. The image of a shallow-buried small object represents the geometric shape of a hyperbola. Therefore, the hyperbola fitting method can be used to estimate the underground wave velocity and to detect the location of the target by imaging Kirchhoff migration and F-K migration are employed. Some of the schemes are discussed in detail.

A. Clutter reduction

Mean removal can be done by using the following equation

$$B_{ave} = B_{raw} - \frac{1}{M}\sum_{i=1}^{M} B_i \quad where \; i = 1 \; to \; M \tag{1}$$

Where B_{raw} is raw data and B_{ave} is mean removed GPR data.

B. Hyperbolic fitting

A point object buried in a subsurface medium will have a hyperbolic signature on b-scan imaging. Therefore, hyperbola fitting procedure can be used to estimate the underground wave velocity. The hyperbola obtained from the B-scan image is governed by the following equation [5].

$$\frac{t^2}{t_0{}^2} - \frac{4(x-x_0)^2}{(vt_0)^2} = 1 \tag{2}$$

where $t_0 = \frac{2z_0}{v}$, z_0 is the depth of target, x_0 is the horizontal position of the target. The above equation is related with the the general quadratic curve equation for hyperbola is given by

$$\frac{y^2}{b^2} - \frac{(x-x_0)^2}{a^2} = 1 \tag{3}$$

where $b = t_0 \; and \; a = \frac{vt_0}{2}$. The wave velocity can be found out by extracting hyperbolic parameters (i.e. a and b) after hyperbola fitting by using

$$v = \frac{2a}{b} \tag{4}$$

C. Kirchoff Migration

In Kirchhoff's migration main aim is to find out the solution to the following wave equation $\varphi(x,z,t)$ within the propagation medium [4], [5]

$$\left(\frac{\partial^2}{\partial x^2} + \frac{\partial^2}{\partial z^2} - \frac{1}{v_m^2}\frac{\partial^2}{\partial t^2}\right)\varphi(x,z,t) = 0 \tag{5}$$

v_m is the velocity of the EM wave inside the medium, calculated as $v/2$ using the "exploding source" model.

The above differential equation is solved by the Kirchhoff integral theorem.

$$P(x,z,t) = \tag{6}$$

$$\frac{1}{2\pi}\int_{-\infty}^{\infty}\left(\frac{cos\theta}{v_m R} \cdot \frac{\partial}{\partial t}P\left(x,z,t-\frac{r}{v_m}\right)\right)dx$$

Where θ the angle of the incident wave to the depth axis (z) and $r = \sqrt{(x-x_m)^2 + z^2}$ is the distance from target at $(x,\, z)$ to observation point $(x_m,\, 0)$.

D. Frequency wave number migration

Frequency wave number migration is also known as stolt migration. It is also based on exploding source model and the scalar wave equation [4], [5].

The algorithm begins with time-domain scalar wave equation for lossless medium

$$\nabla^2\varphi - \frac{1}{v_m^2}\frac{\partial^2\varphi}{\partial t^2} = 0 \tag{7}$$

A mapping procedure is required to transform the data in (k_x, k_z, ω) domain to (k_x, k_z, k_y) domain to be able to use the FFT by using

$$\omega = v_m\left(k_x^2 + k_y^2 + k_z^2\right)^{1/2}$$

$$d\omega = \frac{v_m^2 k_z}{\omega}dk_z$$

The focusing equation can be simplified to a 2D B-scan GPR in the space-depth domain, as shown by the equation

$$F_{FK}(x,z) = \left(\frac{1}{2\pi}\right)^{\frac{3}{2}}\iiint_{-\infty}^{\infty}\frac{v_m^2 k_z}{\omega}P^m(k_x, k_z)$$

$$e^{-j(k_x x + k_z z)}dk_x dk_z \tag{8}$$

Where $P^m(k_x, k_y, k_z)$ is the mapped version of the original data $P(k_x, k_z, \omega)$.

E. PSNR calculation

In image processing, the mean square error (MSE) is used to assess image quality [6]. It is computed by averaging the squared intensities of the original and resultant pixels, i.e.

$$MSE(y,x) = \frac{1}{NM}\sum_{n=0}^{N-1}\sum_{m=0}^{M-1}(x'_{nm} - y'_{nm})^2 \tag{9}$$

x'_{nm} is generated by subtracting GPR image without target from GPR image with target. It only contains target information. y'_{nm} is cluttered reduced image. N –number of sampling points, M-number of A-scans.

$$PSNR = 10log_{10}\frac{s^2}{MSE} \tag{10}$$

Where $s = 255$ for an 8-bit image.

III. SIMULATION AND EXPERIMENTAL RESULTS

To validate the scheme we have gprMax software which is an FDTD software to create the scenario as shown in Fig. 2. For laboratory measurement, we have assembled SFCW GPR system using Vector Network Analyzer (VNA) and horn antenna.

A. Synthetic Experiments

GprMax simulation setup is shown in Fig. 2. In this model, two objects are considered, the first one is a metal pipe and the second one is a metal box like a landmine. Metal pipe with length 6 cm and radius 1.8 cm is located at 30 cm along scan

axis at a depth of 18 cm from the sand surface. The metal cylinder is at 57 cm away from the metal pipe and at depth 23 cm. Antenna scans 127 cm with step size 1 cm along x-axis. 128 A-scans are taken serially to form a B-scan image.
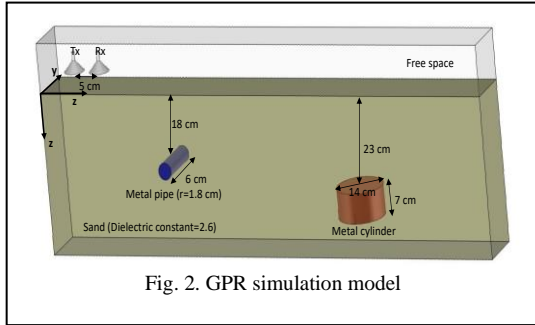

Fig. 2. GPR simulation model

Fig. 3 represents the raw data which consists of static clutter, and target reflections. Due to static clutter, hyperbolic signatures of targets have been faded. Static clutter has been reduced by applying mean removal. Then migration techniques are applied to clutter-reduced data after applying time zero correction and velocity estimation. Kirchhoff migrated image and F-K migrated image are shown in Fig. 4 and Fig. 5 respectively. For performance evaluation, PSNR is calculated. PSNR of Kirchhoff and F-K migrated image is 34.2 and 24.1 respectively.
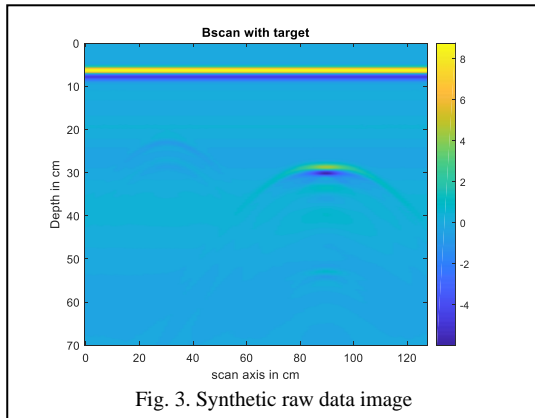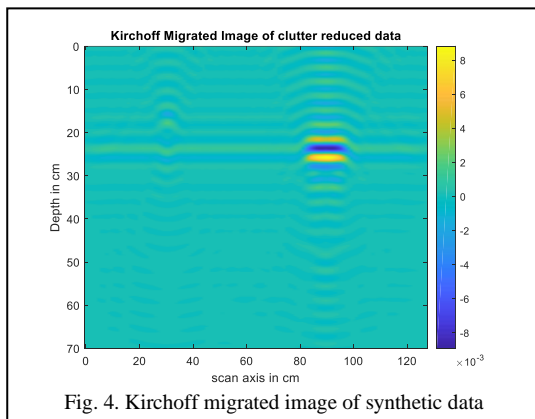

Fig. 3. Synthetic raw data image

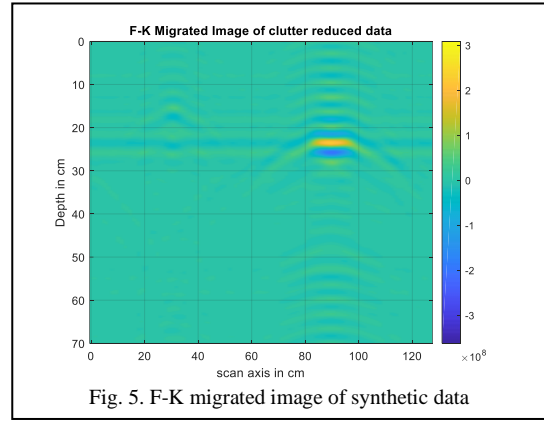
Fig. 4. Kirchoff migrated image of synthetic data

Fig. 5. F-K migrated image of synthetic data

B. Laboratory Experiments

We built an experimental setup using the shape depicted in Fig. 6 to obtain real B-scan GPR readings. Measured data sets are also used to test the performance of the focusing algorithms. This experiment is carried out with the Agilent E5071C ENA Vector Network Analyzer, which creates SFCW signals in the frequency range 9 KHz-4.5 GHz.
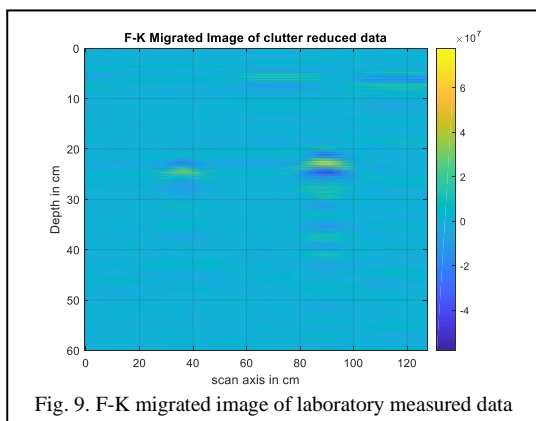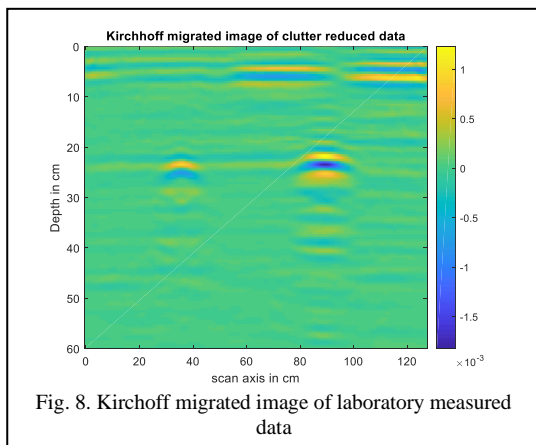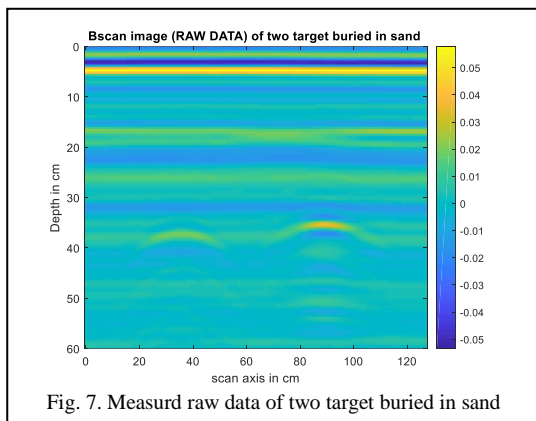

Fig. 6. Laboratory setup for monostatic measurement

In this experiment, we have taken a large wooden box 180 cm×180 cm×40 cm in size as a testbed which is filled with homogeneous dry sand material. The dielectric constant of sand is measured around 2.6 using the velocity estimation method over a frequency range of 1 GHz to 3 GHz. One metal pipe and a mine-like an object i.e. a steel box are considered as targets, and buried at nearly 16 cm and 18 cm respectively from the sand surface. The radius of the metal pipe is 1.8 cm and the length is 50 cm placed horizontally to the scanning axis i.e. x-axis. The steel box is having a radius 7 cm and a length 7 cm is just 57 cm away from the metal pipe.

A B-scan is performed by moving the antenna along the scanning axis, which is perpendicular to the target axis and scanning is done over a synthetic aperture length of 127 cm at 128 spatial points. For each spatial point, the VNA's frequency varies from 0.8 to 4 GHz with step frequency 4 MHz to have 801 discrete points. B-scan GPR image shown in Fig. 7 is obtained by arranging A-scans collected at each spatial point. After clutter-reduction of the B-scan data time zero correction has been applied. Then migration techniques are implemented followed by estimating the correct velocity of the EM wave shown in Fig. 8 and Fig. 9. PSNR values of these KM and F-K migration are 19.8 and 30.2 respectively.

As data is in frequency domain so F-k migration is having good PSNR compared to the Kirchhoff migration.

Fig. 7. Measurd raw data of two target buried in sand

Fig. 8. Kirchhoff migrated image of laboratory measured data

Fig. 9. F-K migrated image of laboratory measured data

IV. CONCLUSION

In this paper, complete imaging schemes are implemented on synthetic as well as laboratory-measured data. Although these migrated images are identical by visual inspection but F-K migration is faster and gives better PSNR as compared to Kirchhoff migration. This scheme is useful for imaging buried objects. However, we need to verify the scheme for different ground scenarios and different targets.

REFERENCES

[1] Hai Liu, Quantitative Characterization of Subsurface Layered Structure by Ground Penetrating Radar, Doctoral dissertation, Graduate School of environmental studies, Tohoku University, Sendai, Japan, 2013.

[2] Behar, V., Vassileva, B. and Kabakchiev, C., A software tool for GPR data simulation and basic processing. Cybernetics and information technologies, 8(4), pp.69-76, 2008.

[3] D. Kumlu and I. Erer, "A comparative study on clutter reduction techniques in GPR images," *4th International Conference on Electrical and Electronic Engineering (ICEEE)*, pp. 323-328, 2017.

[4] Özdemir, C., Demirci, Ş., Yiğit, E. and Yilmaz, B., "A review on migration methods in B-scan ground penetrating radar imaging," Mathematical Problems in Engineering, 2014.

[5] Gilmore, C.G., A comparison of imaging methods using gpr for landmine detection and a preliminary investigation into the sem for identification of buried objects, 2005.

[6] Smitha, N., Bharadwaj, D.U., Abilash, S., Sridhara, S.N. and Singh, V., Kirchhoff and FK migration to focus ground penetrating radar images. International Journal of Geo-Engineering, 7(1), pp.1-12, 2016.

[7] Q. Dou, L. Wei, D. R. Magee and A. G. Cohn, "Real-Time Hyperbola Recognition and Fitting in GPR Data," IEEE Transactions on Geoscience and Remote Sensing, vol. 55, no. 1, pp. 51-62, Jan. 2017.

[8] Z. Lin and W. Jiang, "Estimation on Underground Electromagnetic Wave Velocity Based on Characteristics of Shallow-Buried Small Target Echo," *Fifth International Conference on Instrumentation and Measurement, Computer, Communication and Control (IMCCC)*, pp. 723-726, 2015.